(2)

FINAL TECHNICAL REPORT

Office of Naval Research

Contract N00014-85-K-0527

SEPARATION-BUBBLE VELOCITY MESUREMENTS USING AN OSCILLATING-HOT-WIRE SYSTEM

William S. Saric

Mechanical and Aerospace Engineering
Arizona State University
Tempe, AZ 85287-6106

June 1991

Abstract

A system is developed to allow measurement of both the mean and disturbance flow velocities in separated regions. An oscillating-arm assembly provides a directional bias to the hot-wire probe, along with a linear-step assembly, which steps the probe through the boundary layer. This system is used to investigate the flow field associated with laminar separation bubbles. A series of velocity profiles are measured on an FX63-137 airfoil in the chord-Reynolds-number range: 150,000 $\leq R_c \leq$ 300,000, at angles of attack of $\alpha = 12^o$ and $\alpha = 14^o$. Data are presented on the size of the separation bubble and on the location of transition to turbulence.

Nomenclature

c	=	chord length
H	=	δ^*/θ : shape factor
L	=	length of separation bubble
L_T	=	distance from beginning of separation to transition
R_c	=	$U_o c/\nu$: chord Reynolds number
R_T	=	$U_s L_T/\nu$: transition Reynolds number
t	=	thickness of separation bubble
U_o	=	free-stream velocity
U_s	=	flow velocity at separation
U	=	boundary-layer velocity
V	=	probe velocity
W	=	velocity read by hot wire
x	=	position in chord direction
α	=	angle of attack
δ^*	=	displacement thickness
θ	=	momentum thickness

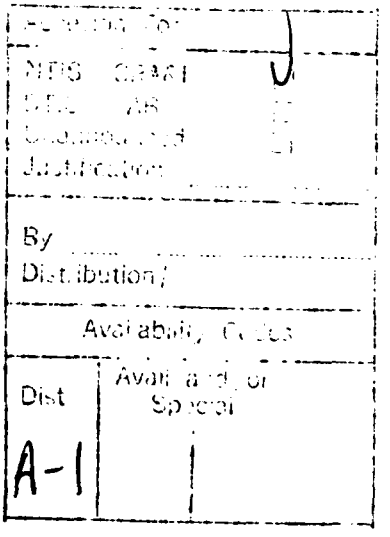

I Introduction

A Motivation

Interests in the use of low-Reynolds-number airfoils has established demands for better qualitative and quantitative understanding of the flow associated with these airfoils. In particular, detailed boundary-layer information is needed to aid in both physical understanding and theoretical development. At the lower range of chord Reynolds numbers, R_c, down to R_c = 10,000, the airfoil performance (measured by lift-to-drag ratio) rapidly deteriorates, as shown by Miley[1]. The drop in performance is due to increased skin friction (thus an increase in the drag) and the fact that the airfoil can behave like a flat plate. To account for the increase in drag, airfoils have been designed with strong adverse pressure gradients to increase lift. These strong adverse pressure gradients, however, stimulate laminar boundary layer separation and violent stall. A thorough review of all aspects of work in this area is given by Mueller[2].

Associated with laminar separation is the formation of a free shear layer. Under most conditions, the inherently unstable character of the free shear layer results in transition to turbulence. In the case where the turbulent shear layer reattaches as a turbulent boundary layer, a separation bubble is formed. With the presence of a separation bubble, lift is maintained and the characteristics of stall are avoided. On the other hand, if velocity disturbance amplitudes are sufficiently high, transition will occur first and separation will be avoided.

Because of the low Reynolds numbers associated with these airfoils, separation is in a laminar boundary layer or a transitional boundary layer. Individually, separation and transition are phenomena that are very sensitive to environmental conditions such as free-stream turbulence, roughness, and noise. Therefore it is important to study the behavior of these airfoils in low-disturbance environments characteristic of flight.

This is clearly a stability problem involving adverse pressure gradients. Although the problem is not new, most earlier work has dealt with a two-dimensional back step geometry (Lochtenberg[3], Browand[4], Roshko[5], Goldstein, Ericksen, Olsen and Eckert[6]) or the exit of axisymmetric free jets (Freymuth[7], Moore[8], Davies and Baxter[9]). More recently, LeBlanc, Blackwelder, and Liebeck[10] have studied the free shear layer resulting from separation over a low Reynolds number airfoil.

In order to develop understanding and to support theoretical work on this problem, it is essential that a data base of detailed velocity profile measurements be established.

Following earlier boundary-layer stability work of Reynolds and Saric[11], done on flat-plate geometries, detailed hot-wire anemometry techniques are used to analyze the low-Reynolds-number airfoil flow.

Special problems, however, are introduced due to the backflow associated with separation. The hot-wire probe is a temperature resistance transducer which is cooled when subjected to flow perpendicular to the wire. Although this assures measurement of velocity in a given plane, the actual direction is not certain. Thus backflow cannot be distinguished from low-speed streamwise flow. When backflow over the probe is present, due to the probe-support structure, the measurements are meaningless. In order to establish a directional bias on the probe, it is necessary to have the probe moving with respect to the model when boundary-layer measurements are taken. This is accomplished by using the oscillating-hot-wire (OHW) configuration that is described below.

B Previous Work

Cantwell[12] first implemented the "flying" hot wire for the study of wakes about a circular cylinder. The flying hot wire was later used to study 2-D separation[13] and 2-D mean flow[14] on an NACA 4412 airfoil (e.g. Wadcock[13] and Coles and Wadcock[14]). Their configuration consisted of a streamlined strut extending into the tunnel. A pancake motor was mounted on the end of the strut with the rotating arms fixed directly to its rotor shaft. Outside of the tunnel the strut was mounted to a slide-assembly vertical traverse which was fixed to a lathe-bed horizontal traverse, allowing two-dimensional positioning control. At the end of each of the arms a hot-wire probe was mounted. In addition, on one of the arms an optical proximity sensor was mounted.

Another flying hot-wire system, developed to measure velocity fields in turbulent wakes, uses an air bearing sled to provide a velocity bias to the hot-wire probe (Watmuff, Perry and Chong[15]). The sled is propelled back and forth by a mechanical spring system. This is mounted above the test section allowing a sting to pass through a slot into the flow. Mounted to the sting is a cross-wire probe which moves along a linear trajectory. In order to keep the sled in motion, energy is put into the system by periodically releasing a compression spring. Once each cycle, the compression spring is compressed and released. A slider-crank type device is used to compress this spring.

In consideration of boundary-layer separation and transition most of the work that has been done has been qualitative in nature. Force measurements have been done by

Volkers[16], Mueller[2], and Marchman[17] among others. These measurements give information about the character of the boundary layer in a "global" way. The hysteresis loop and how it is affected by Reynolds number is an example. Measurements of the surface pressure aid in locating characteristic features of the boundary layer separation, and provide an estimate of the reattachment location. However, only indirect information is obtained on transition. Arena and Mueller[18] and Mueller and Burns[19] have used flow visualization to obtain local, but qualitative, information about the boundary layer and free shear layer. Using hot wires, LeBlanc et al.[10] provide detailed disturbance measurements within the free shear layer. These measurements are correlated to stability calculations, which are based on idealized profiles chosen to match those of the experiment. While providing details of the disturbance, their study did not directly measure backflow velocities.

C Experimental Objectives

It is of primary necessity to measure mean-flow and disturbance-flow velocities in separated boundary-layer flows. Although a LDA system can make mean-flow measurements in separated flows, it cannot measure low-level disturbances. Therefore, a system is needed which will allow the use of hot-wire probes in separated flows. One obvious way to do this is to have the probe moving at the instant of data sampling. To accomplish this goal, Coles Cantwell, and Wadcock[20] developed a flying hot-wire system which used a hot-wire mounted at the end of a rotating arm. Although this rotating hot wire provides the necessary directional bias, slip-ring noise inhibits its use for detailed disturbance-flow measurements where the fluctuating velocities are on the order of 0.1% of the mean flow velocity.

The first consideration is the establishment of the conditions under which the flow separates and reattaches. Secondly, the conditions for which the flow separates and does not reattach, i.e. stalled condition, is to be considered. Of interest in both of these cases is a detailed mapping of the mean flow and disturbance velocities. The mean-flow measurements provide detailed information about the status of the flow throughout the region of interest. Coupled with the mean-flow measurements, disturbance measurements can be used to calculate growth rates in the laminar boundary layer as well as in the free shear layer. Critical amplitudes at separation can also be measured to consider the bearing of these amplitudes on reattachment.

In this series of wind tunnel measurements, however, only mean-flow velocities were measured. Flow unsteadiness in the tunnel, due to a faulty control system, prevented disturbance velocity measurements.

II Wind Tunnel and Model Set-Up

A Wind Tunnel

The entire experiment is carried out at VPI&SU in the Stability Wind Tunnel. Studies have been done (Reynolds and Saric[11]) which show the tunnel to have had good quality flow, with free-stream disturbance levels of 0.02%. However, due to a problem with the propeller speed-control system, mean-flow variations are of the order of 1.0% and higher frequency fluctuations are present with levels to 0.05%. This unsteadiness prevents reliable measurement of disturbance levels within the boundary layer.

The facility is a closed-loop tunnel which uses an air exchange tower for temperature stabilization. The wind tunnel fan is 4.3 m in diameter and has eight constant pitch blades. Seven turbulence screens are positioned before the 5.5 m by 5.5 m settling chamber. The nozzle has a 9:1 area contraction ratio. The test section is 7.3 m long and has a 1.83 m square cross section. A small negative pressure gradient of 0.3%/meter extends down the test section due to the growth of wall boundary layers. To minimize air leakage into the test section, the entire section is enclosed in an airtight control room.

B Model Construction

The test model, constructed at VPI&SU, is a Wortmann FX-63-137-ESM (the designation for smoothing done by Eppler), with a 400 mm chord length and a 1212 mm span. An aluminum "rib" structure is wrapped with a thin aluminum "skin" to achieve the final form. Two 3.2 mm thick endplates fastened to the ends ensure two-dimensional flow around the model. Threaded steel rods extend from the end plates to the mounting fixture.

The ribs are 13.5 mm thick aluminum cut to shape using a numerically controlled milling machine. The trailing edge bottom surface was altered to make it parallel to the top surface. A 3.0 mm thick trailing edge remained instead of a cusp. The ribs are assembled at varied spacing using 9.5 mm steel rods. Holes in the ribs were drilled .03 mm oversized to allow a "slip fit" during assembly. Aluminum rods faced off and drilled, are used for spacers between the ribs. In the central span region, where measurements are taken, the rib spacing is 13 mm with a rib placed at center span. At 109 mm from the center, the spacing is increased to 25 mm. From 300 mm to 606 mm the spacing is 38 mm.

The model skin is 3003 aluminum 0.406 m thick. The aluminum is bonded to the ribs using "Parmacel" two-way tape. At the trailing edge, pop rivets are used between ribs to pinch the top and bottom surfaces together. This is only done in the regions of 25 mm and 38 mm spacing leaving the central region clean. In the immediate area of the rivets, indentations are formed which are filled using a polyester filling putty (Bondo). To obtain a smooth finish, spot putty (Red-Cap) is used.

Once a smooth trailing edge is obtained the whole model is polished, using polishing compound, to remove any surface irregularities. Finally a coat of wax is applied to prevent surface oxidation. The model is then checked for surface variations. The maximum variation is less that 0.3 mm. In the central region where measurements are made surface variations are less than 0.2 mm.

C Model Placement and Movability

The airfoil model is placed vertically in the 1.83 m square test section where a .3 m gap is provided on each end of the model's span, with .61 m gap between the model's "upper surface" and the other side wall. A cross-section view of the test section including the model and the OHW system is shown in Fig. 1.

The entire configuration rests on a steel table below the test section. The table is rotated by a stepping motor with a precision of 0.01 degree. A 75 mm thick steel pipe mounted perpendicular to the table rises into the test section. An aluminum channel (55 mm x 18 mm) is placed 25 mm from the floor and is bolted to the pipe. This channel extends through the wall to a distance of 1.07 m from the center of rotation, at which point the positioning plate is mounted on .68 m steel "legs". This configuration allows the entire OHW system to be rotated with the model to keep the alignment consistent when angle of attack is changed. An aluminum shaft is mounted to the ceiling, at the end of which a thin aluminum bracket is mounted through a radial bearing. With this serving as a model mount, the model can be secure and yet have freedom to rotate.

III OHW Mechanical Details

The oscillating-hot-wire (OHW) mechanical system is built to provide motor-controlled motions of the hot-wire probe in an oscillatory mode and a linear-step mode. The oscillatory motion provides the needed directional bias on the hot-wire probe to allow for measurements in regions of backflow. The linear motion allows the probes to be stepped through the boundary layer to measure boundary-layer profiles. These motions are obtained through the oscillating-arm assembly and the linear-step assembly,

respectively. Chordwise position adjustment is provided to allow profiles to be taken at discrete chord locations. Both the oscillating-arm assembly and the linear-step assembly move together to different positions on the mounting fixture.

A The Oscillating-arm Assembly

The oscillatory motion of the hot-wire probe is generated using a slider-crank device. Fig. 2 shows the oscillating-arm assembly. The hot-wire probe and a distance proximity probe are mounted on the end of an arm which pivots about a fixed-arm pivot shaft. A cylindrical arm-extension rod extends the arm beyond the pivot point. A rotating flywheel, driven by a dc timing motor, transfers the oscillatory motion to the arm. The flywheel has a sliding connector fastened to it through two radial bearings. The arm extension rod slides through the sliding connector, as the flywheel-rotates, while pivoting about the arm pivot shaft. This causes the arm to have one oscillation cycle for one flywheel-rotation cycle, and thus for one motor-rotation period. It should be noted, however, that the duration of the forward sweep of the arm and the duration of the back sweep are different. The forward sweep has a longer duration and a flatter tip-velocity curve. The point at which, the forward moving tip velocity is a maximum is defined as the zero point and is the point at which sampling occurs. This is shown in Fig. 3 which shows the velocity measurement as a function of time. The larger peaks occur during the backward sweep when the probe wake interference is present.

The arm tip consists of a 3 mm thick piece of aluminum mounted perpendicular to the plane of the arm motion. This is fabricated to give a 76.2 mm space between the proximity probe and the hot-wire probe. Ideal-flow calculations of the C_p show the influence of the cylindrical proximity probe at the position of the hot-wire probe to be only 0.27%.

B Linear-Step Assembly

The linear stepping of the hot-wire probe is accomplished by a lead screw pulling a sliding block. The lead screw is turned by a dc stepping motor. The combination of the screw lead and the stepping motor rotation produces a minimum step size of 0.01 mm (although this small a step was never used). The oscillating-arm assembly support is mounted directly to the sliding block. The entire oscillating-arm assembly is moved in order to step the hot-wire probe through a boundary layer. If the system is initially aligned perpendicular to the model surface the linear stepping will result in the zero point always occurring when the hot-wire probe is oriented along the surface normal.

C Chordwise Position Control

The chordwise position control allows the probe to be placed at one of thirty-eight different chord locations. The first location is at $x/c = 0.10$ and the last is $x/c = 0.75$. Between $x/c = 0.10$ and $s/c = 0.375$ the position spacing and $\Delta x/c = 0.0125$, and between $x/c = 0.375$ and $x/c = 0.75$ the position spacing is $\Delta x/c = 0.025$. Figure 4 shows the chordwise sampling grid.

The position control is provided by a mounting fixture which has two series of holes spaced over two curves, which follow the contour of the model. The curves were generated by taking unit normals of the airfoil at the desires x/c. The unit normal was then multiplied by the appropriate distance. This mounting fixture is connected to a beam by four 50 mm steel pipes. This puts the hot-wire probe at the desired spanwise location, centered between the model endplates. The aluminum beam goes through the wind tunnel wall at 25 mm from the floor and bolts to a rotating table under the wind tunnel test section. This is the same beam the model is connected to, assuring alignment through any range of angle of attach.

IV OHW Data Acquisition

The data acquisition is carried out by a MASSCOMP-560 computer using an exterior-source trigger pulse. Both the linear stepping and data sampling are automated. Once a chordwise location is chosen, the linear-step and oscillating-arm assemblies are fixed in place on the positioning plate and a routine is then run on the computer with the result being a boundary-layer profile.

A Triggering

The trigger pulse, which bounds the data sampling, is generated through a series of digital *AND* gates. An encoder, mounted to the motor, produces two 1000 pulse-per-revolution pulse trains which are 180 degrees out of phase. The gating of these two signals produces a 1000 pulse-per-revolution pulse train with a high-level width of 1/4000 of a revolution and a low-level width of 3/1000 of a revolution. This pulse train will hereafter be referred to as "the encoder pulse train."

A reflective transducer is used to produce a one pulse-per-revolution pulse train. The reflective-transducer single pulse-per revolution pulse train is then gated with the 1000 pulse-per-revolution pulse train from the encoder. The final result is a single pulse per revolution which occurs at the zero point.

B Data Sampling

The trigger pulse which occurs when the probes go through the zero point is gated with an internal clock, inside the computer. The internal clock source of the computer is set to provide a continuous 600 kHz pulse train. The result of this final gating is a burst of pulses at a frequency of 600 kHz for a period of 1/4000 revolution. This burst occurs each time the probes go through the zero point. This burst of pulses is then used to trigger the analog-to-digital converter using a data-sampling routine which can sample multiple channels. The two channels are sampled sequentially, one sample for each clock pulse. This feature allows the dc component of the hot-wire probe and a signal from the sweep oscillator to be sampled together, each at 300 kHz.

In order to calculate the mean flow velocity U using a moving hot-wire probe, both the linearized dc voltage from the hot-wire W and the probe velocity V must be known. The mean velocity is calculated by U = W - V. To obtain W and V the linearized dc voltage from the hot-wire probe and a 0.09 Hz sawtooth wave from a sweep oscillator are sampled. The linearized dc voltage from the hot-wire probe is averaged to compute W. To compute V, the data from the sawtooth wave is used. Since the time width of a trigger pulse is small (.25 ms), compared to the period of the sawtooth wave ($\approx$ 11 s), the data from sampling the sawtooth wave over a series of trigger pulses are a series of steps, each step being the width of a trigger pulse. Figure 5 is a diagram showing a typical time series from the linearized dc voltage, and the sweep-oscillator signal. Data sampled from each, over a series of trigger pulses, are shown is Fig. 6.

Using the fact that a radical change in the sampled sweep-oscillator signal represents the start of a new trigger pulse, the data can be separated according to different passes through the zero point. For each burst of data representing a single pass through the zero point, W, V, and U are calculated. To get a time average, the U calculated from several passes can be averaged.

Once the data are broken into different bursts, the data analyses can be done. Averaging the linearized dc voltage over one burst gives the value of W. To get the value of V, the actual probe velocity, the rate of rotation of the flywheel must be calculated. Counting the number of samples per burst and knowing the frequency of sampling, the time increment of a burst is calculated. Using this time increment and the distance travelled (1/4000 revolution) the angular velocity is calculated. Finally the probe velocity is calculated using the angular velocity and the appropriate kinematic relationships.

Once the mean flow and disturbance velocity profiles are measured with the probe in motion, an additional disturbance velocity profile can be measured with the probe not in motion. Due to the short duration of sampling when the probe is in motion, only higher frequency disturbances can be resolved. Since the frequencies of interest for boundary-layer instabilities are much lower, the probe is held fixed during disturbance measurements. After sequentially measuring a mean-flow profile and a disturbance profile, the mean-flow profile is used to determine the range of validity of the disturbance profile. Therefore the entire flow field can be mapped throughout the free shear layer.

C Distance Measurement

In order to spatially correlate the velocities measured with the hot-wire probe, the initial normal distance of the probe from the model must be determined. Once the initial distance is known, the distances of the entire series of velocities measured is calculated by using the number of steps taken between velocity readings. A proximity probe with a signal conditioner is used to measure the initial distance. The probe is set up to produce a voltage (0.0 - 3.0 V) linearly proportional to the distance of the probe from the model. The linear measuring range is from 0.0 - 1.1 mm. What is required, however, is the distance of the hot-wire probe from the model. A calibration of the proximity probe is done so that a voltage reading from the proximity probe will define the distance of the hot-wire probe.

To calibrate the proximity probe the OHW system was set at a chord position where there is a zero pressure gradient. In many cases a slight favorable or adverse gradient is used for Reynolds number and angle of attack conditions in which there is no zero gradient. With the chordwise position set, the OHW is locked in the zero point and stepped into the boundary layer. A routine is then run which steps the probes out of the boundary layer, measuring the velocity and the proximity-probe voltage. The routine then uses the almost linear portion of the velocity profile and extrapolates to locate the model. The slope of intercept are then calculated which defines a line that relates the hot-wire probe position to the proximity probe voltage. Then the probe can be used at any location in the presence of pressure gradients. Each time the model is moved, the calibration is repeated.

V Measurements

A OHW Documentation

In order to determine the reliability of the OHW system and to investigate any limitation of the system a series of detailed measurements are made. The first measurement of interest is a time series of the linearized dc voltage form the hot-wire probe when the arm is moving. Other measurements considered are the velocities measured with the arm in motion versus velocities measured with the arm fixed. Fixing the arm using a steel pin, the wind-tunnel conditions are set and the linearized dc voltage from the hot-wire probe is measured. Under the same conditions with the arm in motion the linearized dc voltage is measured and the velocity is calculated. The variation is less than 1.0% which as mentioned before, is of the order of the free-stream fluctuations. Boundary-layer profiles, measured with the arm fixed and in motion show very good agreement. The details are given by *Crouch*[21].

B Laminar Separation Bubble

With the OHW system calibrated, a detailed investigation of the flow quality, which includes the measurement of disturbance amplitudes and spectra, is done. Finding the disturbance amplitudes to be higher than usual for this tunnel, 0.05% as opposed to 0.02%, velocity time series are measured. These time series indicate a low-frequency unsteadiness of the order of 1% as shown in Fig. 7. With this unsteadiness in the flow and its influence on the disturbance amplitudes, it is impossible to do any of the detailed disturbance measurements that provide information about the breakdown mechanism to transition. Long time averages were made of the mean flow to obtain meaningful data.

Also of interest are the characteristics of the upper and lower branches of the hysteresis loop found in the C_L vs α curve. The velocity profiles on the lower branch for conditions of R_c = 200,000 and $\alpha = 12^o$ are measured. A profile taken at x/c = 0.475 suggests the model to be stalled. However, transition always occurs (resulting in reattachment) before any detailed measurements can be made. It is thought that the unstable nature of the free shear layer is only part of the reason the lower branch conditions cannot be maintained. With stalled conditions the "effective model section" is increased and wall affects may become important. Moreover, unsteady fluctuations, like those present in the tunnel are known to effect the free shear layer.

Realizing the potential for false information on lower-branch measurements, attention is focused on the upper branch, paying particular attention to the separation bubble. The separation bubble is defined to be the region of recirculation. The "separation streamline" is determined by integrating the velocity profiles to the point at which the backflow is balanced by the forward flow. Figure 8 shows a series of mean-velocity

profiles measured at $\alpha = 14^o$ and $R_c = 150{,}000$. Separation occurs at x/c = 0.15. The bubble (shown with the solid line) then grows with a strong backflow present. At x/c = 0.30, transition (defined as the start of large fluctuations in the flow velocity) occurs. From this point the bubble closes, finally reattaching at x/c = 0.35. The maximum bubble thickness is 1.79 mm which occurs at 75% of the bubble length.

Figure 9 shows a series of profiles for $\alpha = 14^o$ and $R_c = 200{,}000$. For this case the flow separates at about x/c = 0.16. The bubble grows from this point with transition occurring at x/c = 0.27 and reattachment at x/c = 0.30. The maximum bubble thickness is 0.62 mm. Figure 10 shows a series of profiles for $\alpha = 14^o$ and $R_c = 250{,}000$. Separation occurs at x/c = 0.175. The bubble grows until transition, at x/c - 0.275. The maximum thickness of the backflow region is 0.4 mm and occurs at about 75% of the bubble length. The full extent of the bubble can not be determined due to a lack of data points in this region.

The final case with $\alpha = 14^o$ is given in Fig. 11 for $R_c = 300{,}000$. The flow separates at x/c = 0.20. The bubble then grows, transition occurs, and the flow reattaches at x/c = 0.26. Due to the small size of the bubble and the lack of profiles in this region, no chordwise details can be determined. However, the maximum thickness of the backflow region is found by interpolation to be 0.25 mm.

For the case of $\alpha = 12^o$ and $R_c = 200{,}000$ profiles are shown in Fig. 12. The flow separates at x/c = 0.25. The bubble then grows with an increasing strength of backflow. Transition occurs at x/c = 0.40 followed by reattachment at x/c = 0.45. The maximum bubble thickness, which occurs close to 75% of the bubble length, is 1.60 mm. The final series of profiles measured, shown in Fig. 13, is for $\alpha = 12^o$ and $R_c = 250{,}000$. Separation occurs at x/c = 0.275. The bubble grows until about x/c = 0.37, where transition occurs. Reattachment follows at x/c = 0.40. The maximum bubble thickness is 0.59 mm and it occurs at 75% of the bubble length.

Finally, the boundary-layer profiles are integrated to provide quantitative information for numerical study. Displacement thicknesses, momentum thickness, and shape factors are given in Table 1. Table 2 gives a summary of the separation bubble and transition data.

C Transition of the Free Shear Layer

The transition location, marked by the onset of large fluctuations in the velocity, occurs at approximately the same location as the maximum bubble thickness. Transition Reynolds numbers are calculated in the cases for which sufficiently detailed information is available. The transition Reynolds number, R_t, is defined by $U_s L_T/\nu$ where U_s is the edge velocity at the onset of separation and L_T is the distance from the beginning of separation to the beginning of transition. For the case $\alpha = 12^o$ R_T = 58,000 at R_c = 200,000 and R_T = 54,000 at R_c = 250,000. For $\alpha = 14^o$, where the airfoil is at incipient stall, R_T = 33,000 at R_c = 150,000 and R_T = 37,000 at R_c = 200,000. The Transition Reynolds numbers are only accurate within 5,000 due to the error introduced by the chordwise spacing of the measurement grid. Therefore, there is no significant dependence of R_T on R_c. The value of R_T at $\alpha = 12^o$ agrees quite well with correlations of transition as a function of free-stream turbulence (see Davis, Carter, and Reshotko[22]).

VI Conclusions

The OHW system is found to accurately measure boundary-layer and free-shear-layer velocity profiles. Due to the amount of time required to measure each profile, however, care must be taken to maintain good calibration when flow conditions are changing.

Measurements of separation bubbles show that the maximum bubble thickness occurs at about 75% of the bubble length. For $\alpha = 14^o$ and $R_c = 150,000$ the bubble thickness to length ratio t/L, is 2.2%. For $\alpha = 12^o$ and R_c = 200,000 t/L = 2.0%. For all other cases considered, t/L ranged from 0.9% to 1.2%. The effect of change in Reynolds number on the bubble is greater for lower Reynolds numbers then for higher. For the case of $\alpha = 14^o$ a change in R_c from 150,000 to 200,000 resulted in a change in bubble thickness of 1.1 mm. The length is changed by 6% of the chord length. Changing R_c from 200,000 to 250,000, however, results in only $\simeq 0.1mm$ change in bubble thickness. The bubble length is changed by 3% of the chord length.

Measurements show that the separation bubble moves downstream and is reduced in size with increasing Reynolds number. Separation is delayed and transition is accelerated. This suggests that critical disturbance amplitudes for transition are reduced or that the disturbances within the boundary layer are larger.

One explanation of this is that by delaying separation, disturbances have more time to grow in the boundary-layer environment. Therefore some critical amplitude at separation would be reached. From this point transition is inevitable, and the location

is set. If the critical amplitude at separation is not reached, then transition does not occur and turbulence results from the breakdown of the free shear layer. In the event that the critical amplitude for transition occurs before separation, transition occurs and separation is avoided.

Acknowledgements

This work was supported by the Office of Naval Research, Contract No. N00014-84-K-0093 and N00014-85-K-0527.

References

1. Miley, S.J. "An analysis of the design of airfoil sections for low Reynolds numbers," Ph.D. Thesis, Mississippi State Univ., (1972).

2. Mueller, T.J. "Low Reynolds number vehicles," AGARD-AG-288, (1985)

3. Lochtenberg, B.H. "Transition in a separated laminar boundary layer," J. Aero. Sci., pp. 92-96, (1960)

4. Browand, F.K. "An experimental investigation of the instability of an incompressible separated shear layer," J. Fluid Mech., Vol. 26, Part 2, pp. 281-307, (1966).

5. Roshko, A. "Transition in incompressible near wakes," Phys. Fluids Suppl: Boundary Layers and Turbulence, pp. S181-S182, (1967).

6. Goldstein, R.J., Ericksen, V.L., Olsen, R.M., & Eckert, E.R.G. "Laminar separation reattachment and transition of flow over a downstream-facing step," ASME Paper 69-WA/FE-5, (1969).

7. Freymuth, P. "On transition in a separated laminar boundary layer," J. Fluid Mech., Vol. 25, Part 4, pp. 683-704, (1966).

8. Moore, C.J. "The effect of shear layer instability on jet exhaust noise," Lecture Notes Physics, No. 76, Vol. 2, Springer-Verlag, pp. 254-264, (1978).

9. Davies, P.L. & Baxter, D.R.J. "Transition in free shear layers," Lecture Notes Physics, No. 76, Vol. 1, Springer-Verlag, pp. 124-135, (1978).

10. LeBlanc, P., Blackwelder, R., & Liebeck, R. "A comparison between boundary layer measurements in a laminar separation bubble flow and linear stability theory calculations," Lecture Notes Engineering, No. 54, Vol. 1, Springer-Verlag, pp. 189-205, (1989).

11. Reynolds, G.A. & Saric, W.S. "Experiments on the stability of the flat-plate boundary layer with suction," AIAA J. Vol. 2, (1986) (also AIAA Paper No. 82-1026).

12. Cantwell, B.J. "A flying hot-wire study of the turbulent near wake of a circular cylinder at a Reynolds number of 140,000" Ph.D. Thesis, Caltech, (1975).

13. Wadcock, A.J. "Flying-hot-wire study of two-dimensional turbulent separation on an NACA 4412 airfoil at maximum lift," Ph.D. Thesis, Caltech, (1978).

14. Coles, D., & Wadcock, A. "Flying-hot-wire study of 2-D mean flow past a NACA 4412 airfoil at maximum lift," Tech. Rep. to NASA-Ames (Grants NGL 05-002-229 & NSG-2319), (1978).

15. Watmuff, J.H., Perry, A.E., & Chong, M.S. "A flying hot-wire system," Exp. Fluids, pp. 63-71, (1983).

16. Volkers, D.F. "Preliminary results of wind tunnel measurements on some airfoil sections at Reynolds numbers between 60,000 and 500,000," Delft Tech. Univ., Memorandum M-276, Netherlands, (1977).

17. Abtahi, A.A., & Marchman, J.F. "Aerodynamics of an aspect ratio 8 wing at low Reynolds numbers," AIAA Paper No. 85-0278, (1985).

18. Arena, A.V. & Mueller, T.J. "On the laminar separation, transition, and turbulent reattachment of low Reynolds number flows near the leading edge of airfoils," AIAA Paper No. 79-0004, (1979).

19. Mueller, T.J. & Burns, T.F. "Experimental studies of the Eppler 61 airfoil at low Reynolds numbers, " AIAA Paper no. 82-0345, (1982).

20. Coles, D., Cantwell, B., & Wadcock, A. "The flying hot wire and related instrumentation," Tech. Rep. to NASA-Ames, (Grant NGL 05-002-229), (1977).

21. Crouch, J.D. "An Oscillating Hot Wire for Measurements in Separated Flows," M.S. Thesis, VPI&SU, (1985).

22. Davis, R.L., Carter, J.E., & Reshotko, E., "Analysis of Transitional Separation Bubbles on Infinite Swept Wings", AIAA Paper No. 85-1685, (1985).

Table 1

α = 14° R_c = 150,000 U_∞ = 6.06 m/s

x/c	δ^*	θ	H
0.112	1.46mm	0.60mm	2.44
0.150	2.28	0.53	4.28
0.200	2.12	0.36	5.97
0.250	3.14	0.23	13.82
0.300	3.21	0.20	16.40

α = 14° R_c = 150,000 U_∞ = 6.22 m/s

x/c	δ^*	θ	H
0.325	2.81mm	0.46mm	6.14
0.350	2.40	0.61	3.91
0.400	1.71	0.83	2.07
0.450	1.35	0.85	1.59

α = 14° R_c = 200,000 U_∞ = 8.02 m/s

x/c	δ^*	θ	H
0.150	1.59mm	0.58mm	2.76
0.200	1.63	0.44	3.67
0.250	2.22	0.40	5.51
0.300	1.97	0.53	3.71
0.350	1.17	0.62	1.90
0.400	1.12	0.72	1.55

α = 14° R_c = 250,000 U_∞ = 10.47 m/s

x/c	δ^*	θ	H
0.112	0.91mm	0.43mm	2.19
0.150	1.06	0.33	3.18
0.175	1.33	0.40	3.31
0.200	1.55	0.41	3.80
0.250	2.02	0.45	4.49
0.262	1.84	0.47	3.88
0.275	1.48	0.57	2.61
0.288	1.55	0.58	2.68
0.300	1.14	0.60	1.90
0.350	1.10	0.60	1.85

α = 14° R_c = 300,000 U_∞ = 12.34 m/s

x/c	δ^*	θ	H
0.112	0.64mm	0.38mm	1.71
0.175	1.11	0.35	3.20
0.200	1.29	0.40	3.24
0.225	1.51	0.39	3.89
0.250	1.15	0.42	2.72
0.300	0.77	0.49	1.56
0.350	0.74	0.53	1.39

α = 12° R_c = 200,000 U_∞ = 7.94 m/s

x/c	δ^*	θ	H
0.250	1.80mm	0.49mm	3.66
0.275	1.84	0.48	3.81

α = 12° R_c = 200,000 U_∞ = 8.0 m/s

x/c	δ^*	θ	H
0.312	2.03mm	0.44mm	4.60
0.375	2.87	0.32	9.01
0.425	2.81	0.41	6.81
0.450	2.55	0.60	4.23
0.475	1.97	0.78	2.52

α = 12° R_c = 250,000 U_∞ = 10.58 m/s

x/c	δ^*	θ	H
0.200	1.09mm	0.43mm	2.52
0.250	1.54	0.47	3.28
0.275	1.69	0.47	3.62
0.300	1.92	0.47	4.11
0.350	2.09	0.47	4.43

α = 12° R_c = 250,000 U_∞ = 10.46 m/s

x/c	δ^*	θ	H
0.362	2.16mm	0.42mm	5.17
0.375	2.34	0.48	4.91
0.400	2.16	0.49	4.37
0.425	1.63	0.64	2.55
0.450	1.25	0.69	1.81

Table 2

Summary of Separation Bubble Data

$\alpha = 14°$						
R_c	$(x/c)_s$	$(x/c)_T$	$(x/c)_r$	L(mm)	t_{max}(mm)	t/L
150,000	0.15	0.30	0.36	80.	1.79	2.2
200,000	0.16	0.27	0.30	56.	0.62	1.1
250,000	0.175	0.26	0.29	44.	0.40 *	0.91 *
300,000	0.20	0.24	0.26	24.	0.25 *	1.0 *
$\alpha = 12°$						
R_c	$(x/c)_s$	$(x/c)_T$	$(x/c)_r$	L(mm)	t_{max}(mm)	t/L
200,000	0.25	0.40	0.45	80.	1.60	2.0
250,000	0.275	0.363	0.40	50.	0.59	1.2

*: maximum thickness based on back flow only

Note: $(x/c)_{t_{max}} \simeq (x/c)_T$

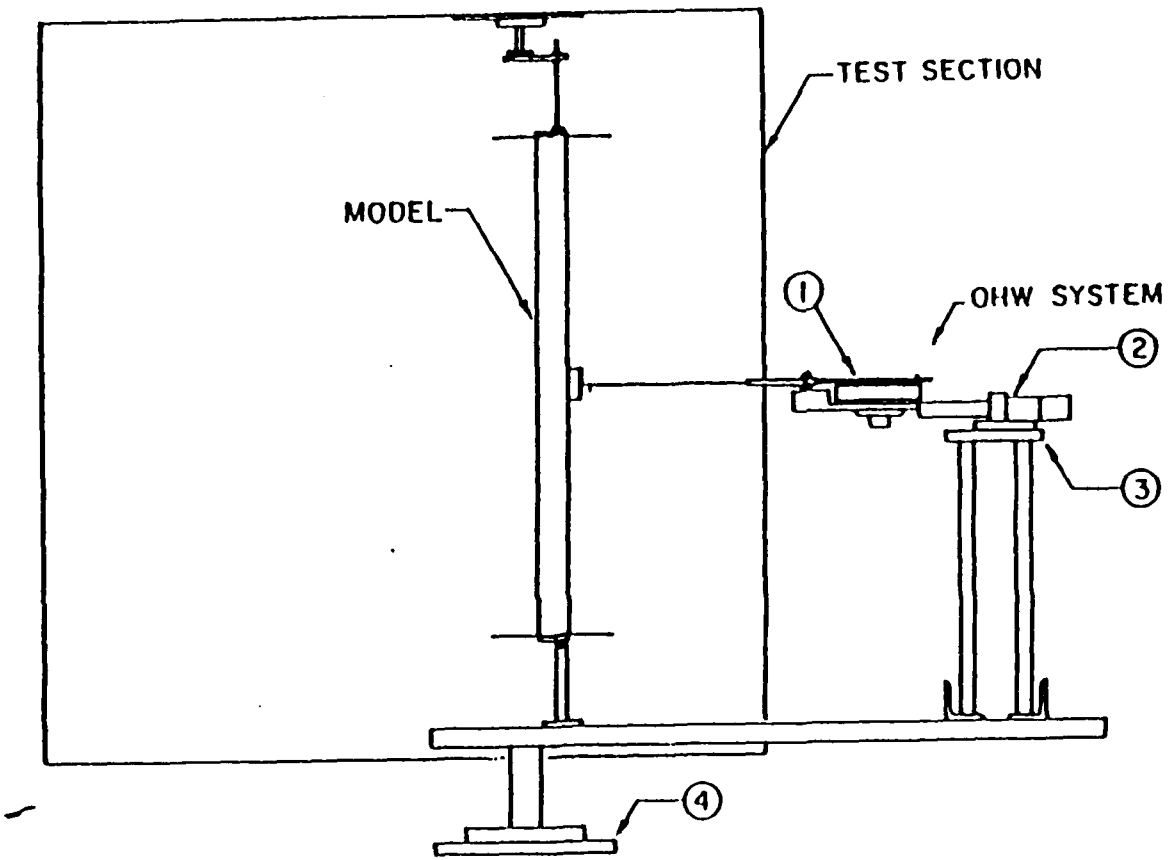

Figure 1. Placement of Model and OHW System in Wind Tunnel: (1) oscillating arm assembly; (2) linear step assembly; (3) positioning plate; (4) rotating table.

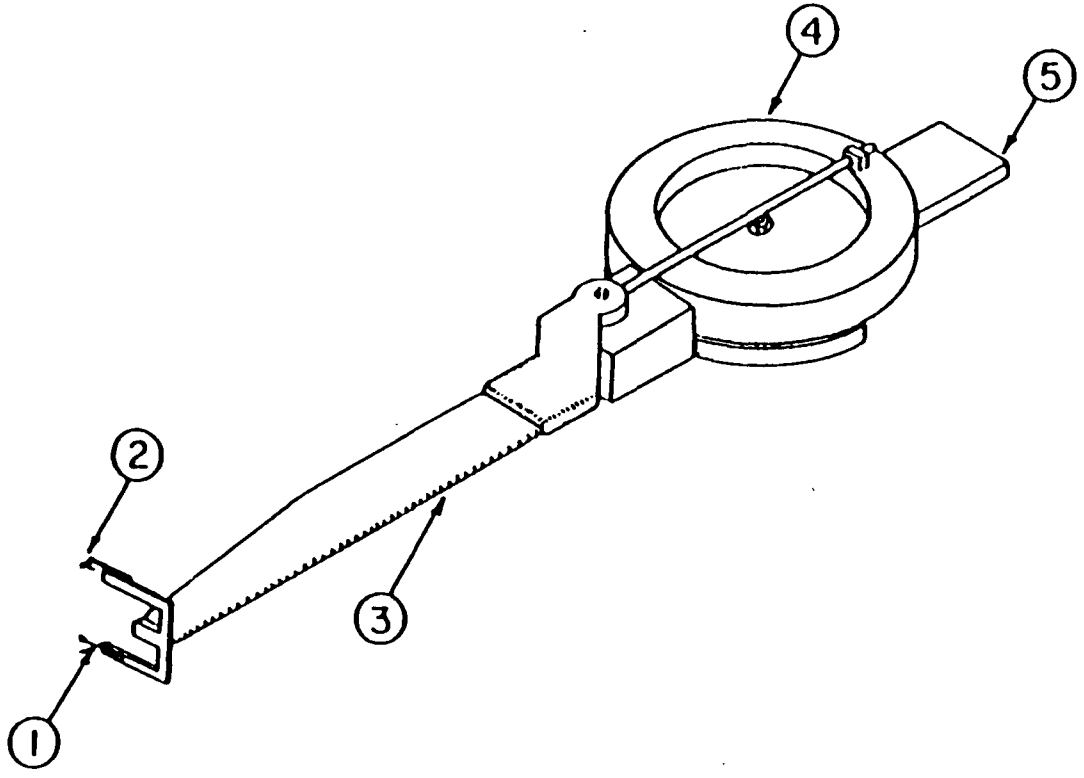

Figure 2. Oscillating Arm Assembly: (1) hot-wire probe; (2) proximity probe; (3) oscillating arm; (4) flywheel; (5) assembly support.

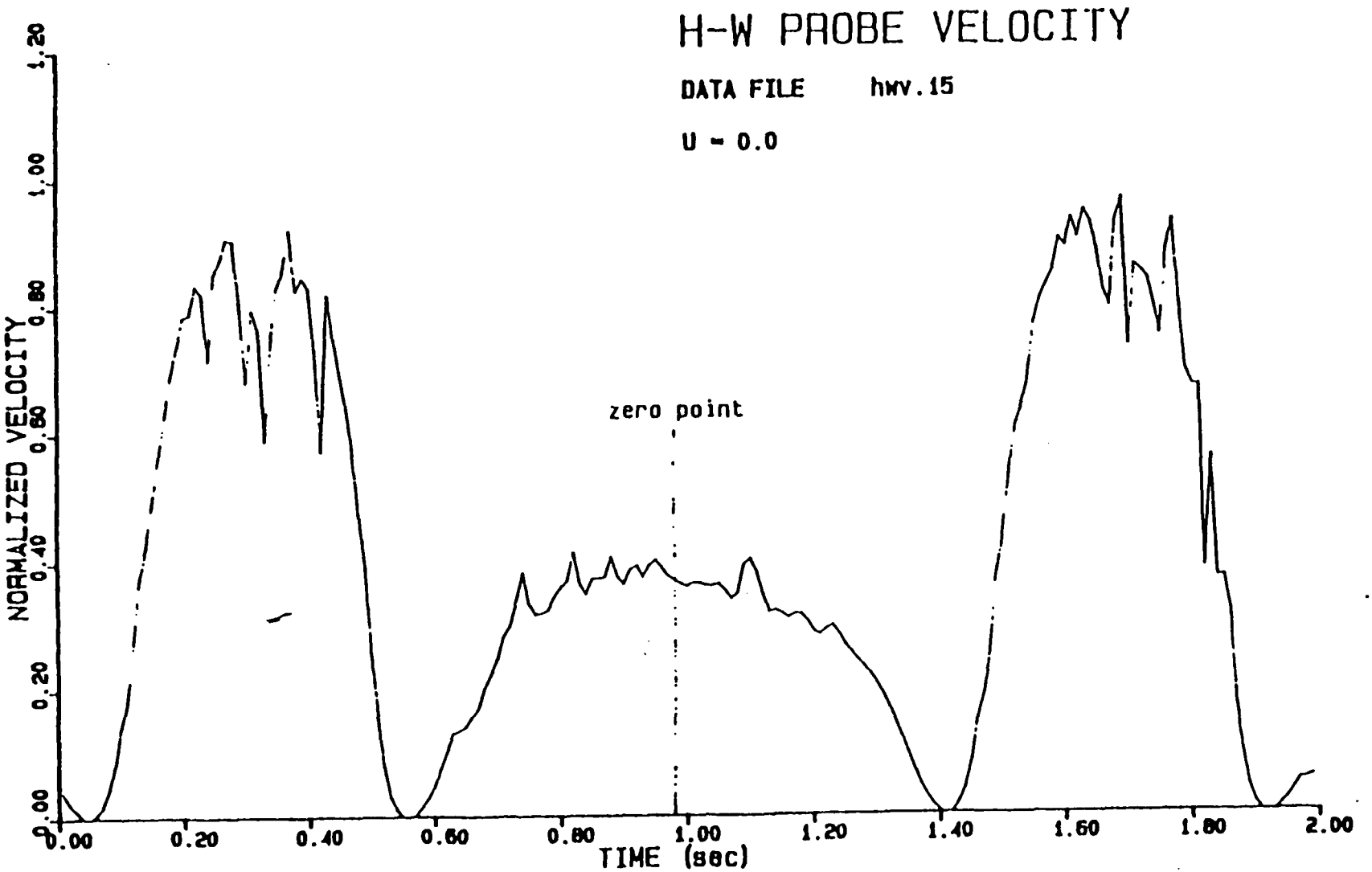

Figure 3. Hot-Wire Output: Time series showing the zero point.

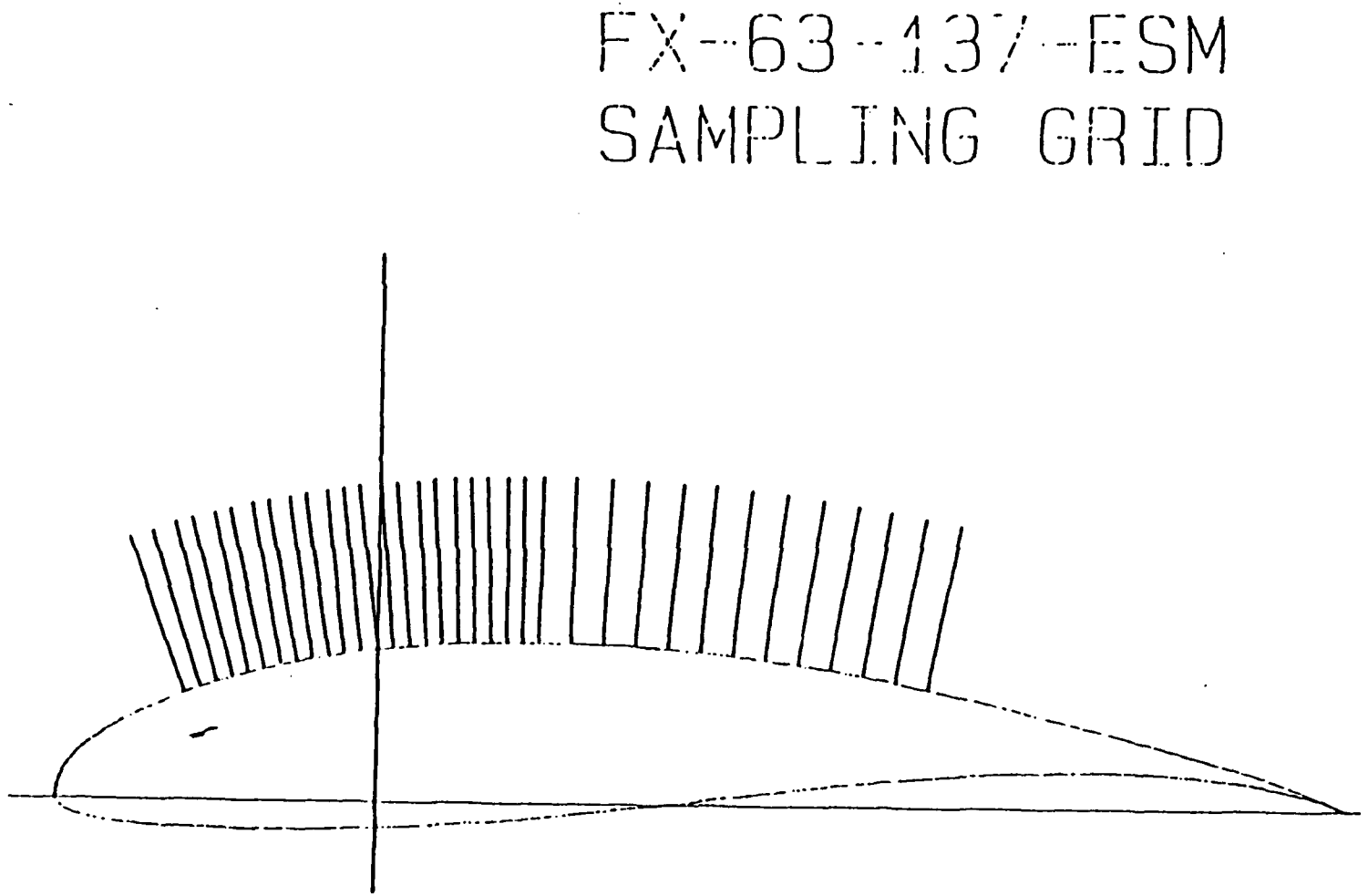

Figure 4. Chordwise Sampling Grid

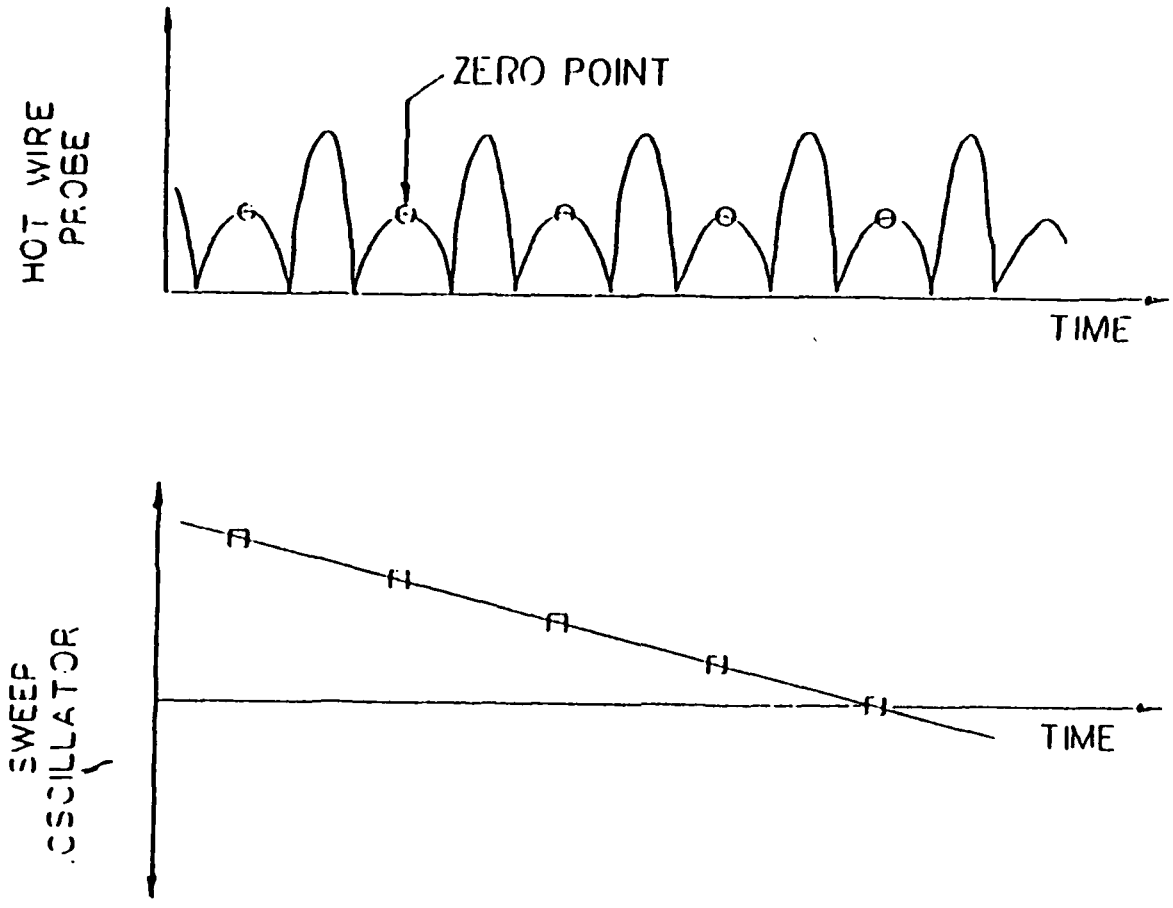

Figure 5. Linearized Hot-Wire and Sweep Oscillator Output: Data taken when arm is in motion.

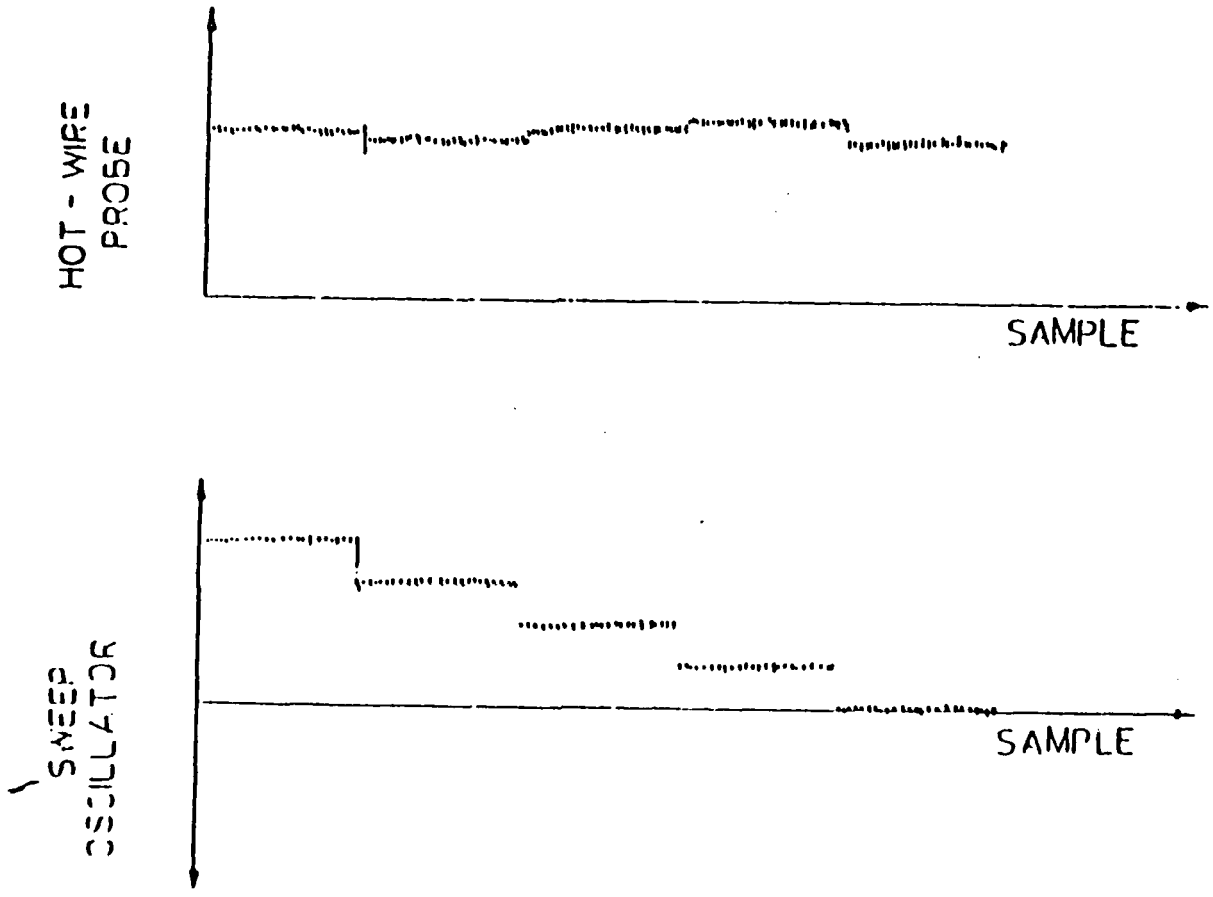

Figure 6. Linearized Hot-Wire and Sweep Oscillator Output: Data are digitized over a series of trigger pulses when the arm is in motion.

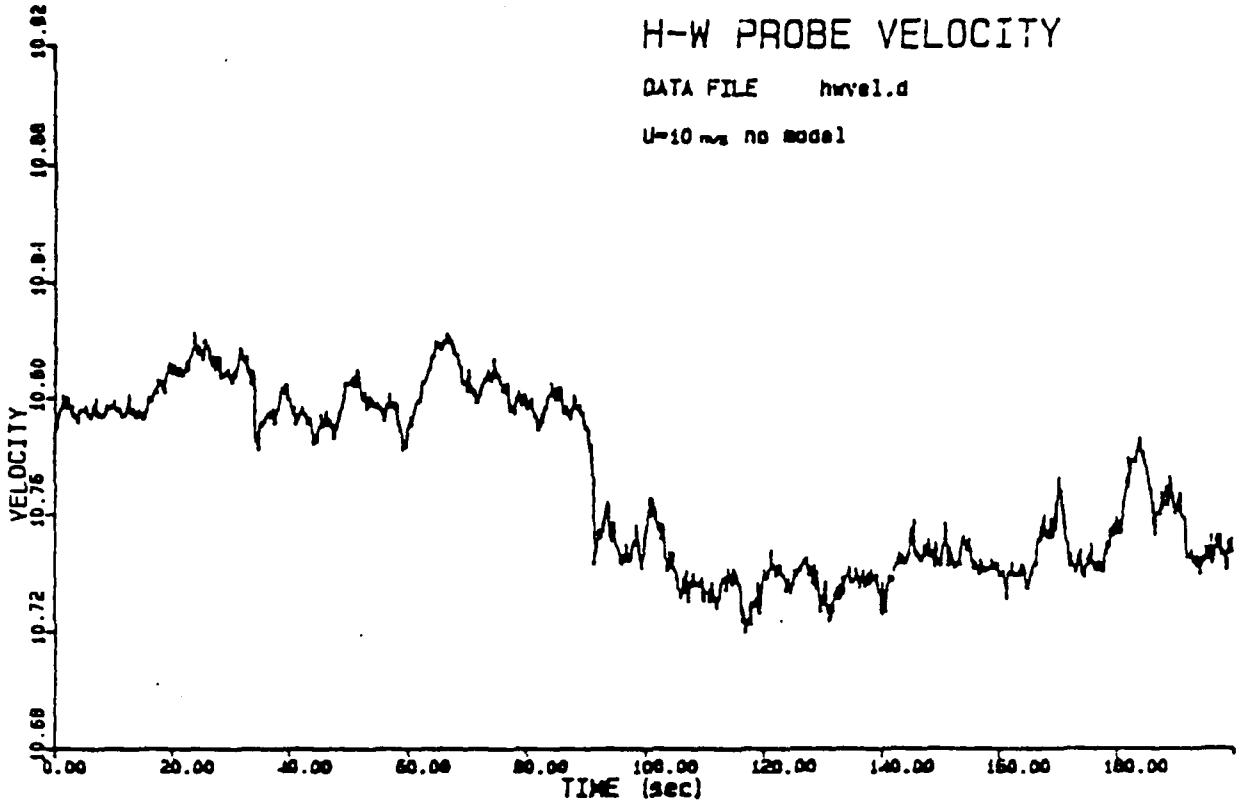

FIGURE 7. Tunnel Velocity vs Time: The arm is fixed and no model is in the flow.

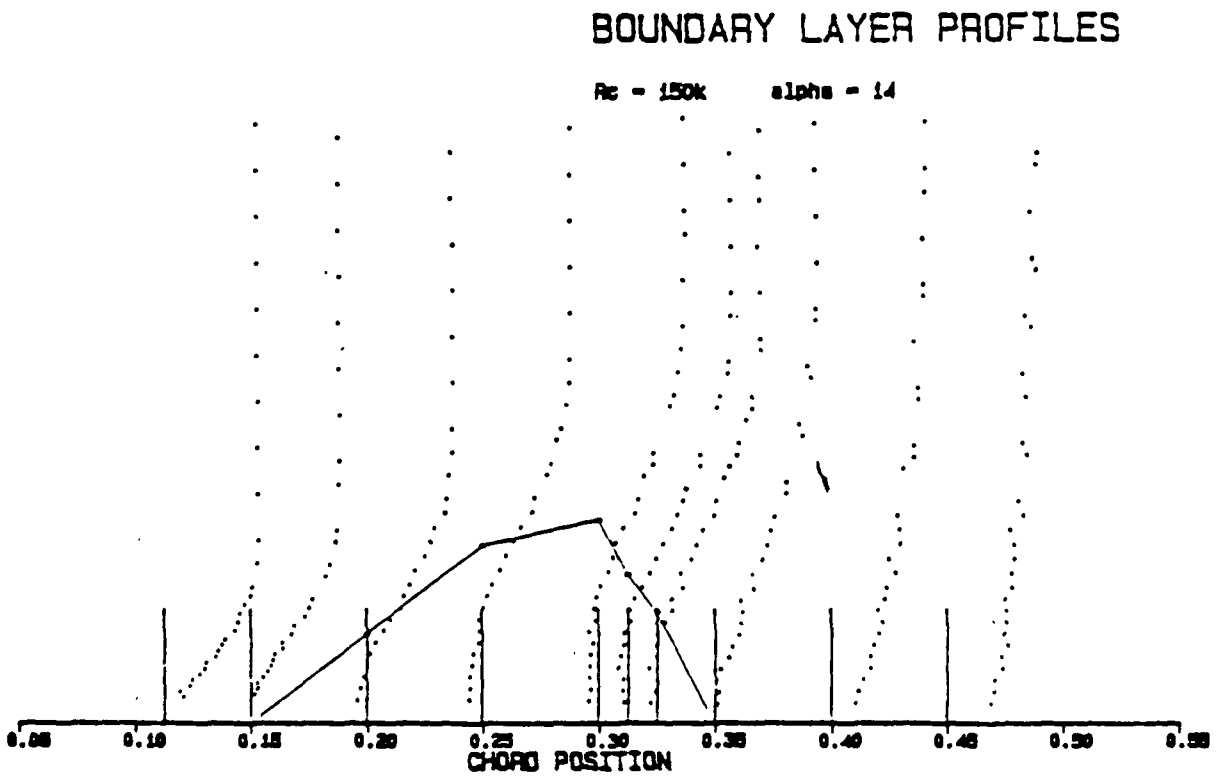

FIGURE 8. Velocity Profiles for $\alpha = 14°$, $R_c = 150,000$.

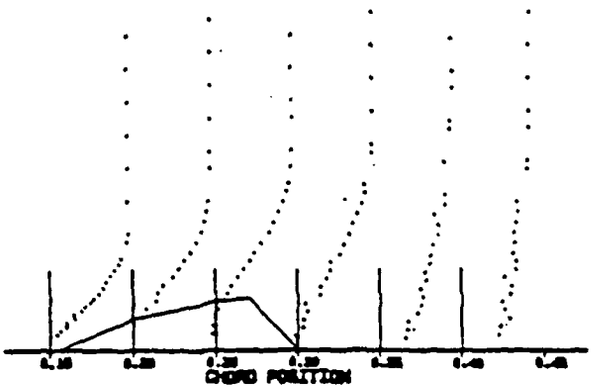

FIGURE 9. Velocity Profiles for α = 14°, R_c = 200,000.

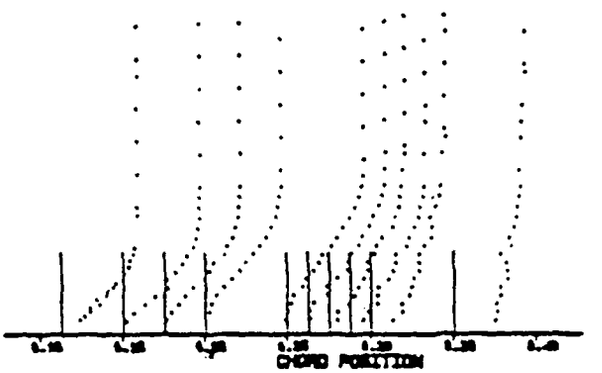

FIGURE 10. Velocity Profiles for α = 14°, R_c = 250,000.

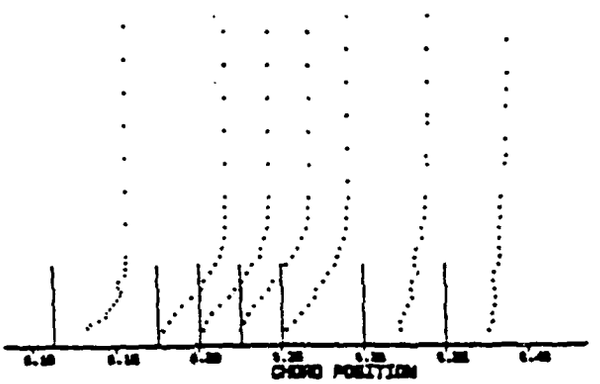

FIGURE 11. Velocity Profiles for α = 14°, R_c = 300,000.

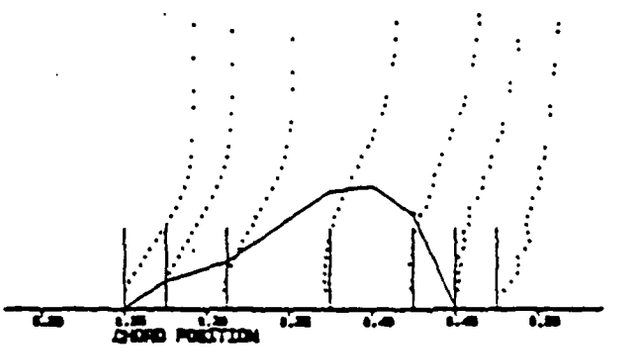

FIGURE 12. Velocity Profiles for α = 12°, R_c = 200,000.

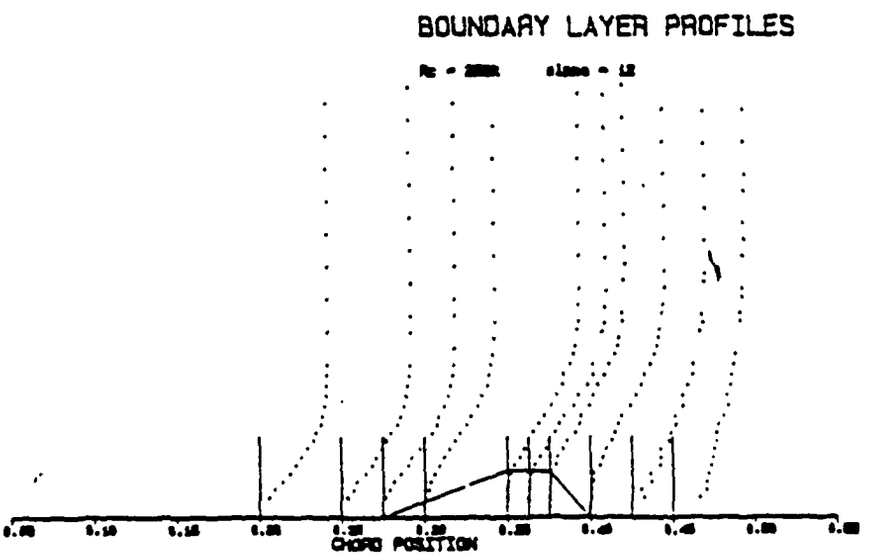

FIGURE 13. Velocity Profiles for α = 12°, R_c = 250,000.